Asian Journal of Physical and Chemical Sciences

3(2): 1-15, 2017; Article no.AJOPACS.35528
ISSN: 2456-7779

A Blood Flow Model of a Bifurcating Artery

W. I. A. Okuyade[1*] and T. M. Abbey[2]

[1]Department of Mathematics/Statistics, University of Port Harcourt, Port Harcourt, Nigeria.
[2]Applied Mathematics and Theoretical Physics Group, Department of Physics, University of Port Harcourt, Port Harcourt, Nigeria.

Authors' contributions

This work was carried out in collaboration between both authors. Both authors read and approved the final manuscript.

Article Information

DOI: 10.9734/AJOPACS/2017/35528
Editor(s):
(1) Ahmed Abdel-latif, Department of Mathematics and Engineering Physics, Faculty of Engineering, Fayoum University, Fayoum, Egypt.
Reviewers:
(1) John Abraham, University of St. Thomas, USA.
(2) Dipak Kumar Mandal, College of Engineering and Management, India.
(3) Satyasaran Changdar, Institute of Engineering & Management, India.
Complete Peer review History: http://www.sciencedomain.org/review-history/21260

Original Research Article

Received 17th July 2017
Accepted 14th August 2017
Published 6th October 2017

ABSTRACT

A flow model of blood in a normal bifurcating artery is presented. The models of the problem are solved using the regular perturbation series expansion. Solutions of the temperature, concentration, velocity, Nuselt number, Sherwood number and skin friction are realized, and presented quantitatively and graphically using the Maple 18 computational software. It is noticed, among others, that the increase in Grashof number increases the temperature, velocity, Nusselt number, Sherwood number and wall shear stress, whereas the Hartmann number increases the concentration but decreases the temperature, velocity and wall shear stress. These results have some attendant physiologic implications on the well-being of man.

Keywords: Arterial model; blood flow; bifurcation; magnetic field; convective flow.

**Corresponding author: E-mail: wiaokuyade@gmail.com;*

NOMENCLATURES

C' : Concentration (quantity of material being transported)
D : Diffusion coefficient
g : Gravitational field vector
Gc : Grashof number due to concentration difference
Gr : Grashof number due to temperature difference
K : constant body temperature
K_1 : a constant
p' : Fluid pressure
p : Dimensionless pressure
Pr : Prandtl number
Q : Heat absorption coefficient
Re : Reynolds number,
Sc : Schmidt number
T' : Fluid temperature
(u, w') : Velocity components of the fluid in the mutually orthogonal axes
(u, w) : Non-dimensionalized velocity components
(r', x') : Mutually orthogonal axes
(r, x) : Dimensionless orthogonal axes
α, β : Bifurcation angles
ρ' : Density of the fluid
ρ : Dimensionless density of the fluid
μ : Viscosity of the fluid
μ_m : Magnetic permeability of the fluid
κ : Permeability of the porous medium
σ_e : Electrical conductivity of the fluid
υ : Kinematic viscosity of the fluid
χ^2 : Local Darcy number
δ_1^2 : Rate of chemical reaction
Θ : Dimensionless temperature
$\Re$: Aspect ratio
Φ : Dimensionless concentration
B_c : Volumetric expansion coefficient due to concentration
B_o^2 : Applied uniform magnetic field strength
B_t : Volumetric expansion coefficient due to temperature
C_p : Specific heat capacity at constant pressure
C_w : Constant wall temperature maintained
C_∞ : Concentration at equilibrium
k_o : Thermal conductivity of the medium
k_r^2 : Rate of chemical reaction
ℓ_c : Scale length
M^2 : Hartmann's number
N^2 : Heat exchange parameter
Pe_h : Peclet number due to heat transfer
Pe_m : Peclet number due to mass transfer
p_∞ : Ambient/equilibrium pressure
T_w : Constant wall concentration at which the channel is maintained
T_∞ : Temperature at equilibrium
U_o : Characteristic velocity of the flow

1. INTRODUCTION

The study of arterial blood flow under diseased and normal physiologic conditions is very significant as most deaths arise from cardiovascular diseases, which may be associated with abnormal blood flow.

Nutrients and wastes transport round the body is the main function of the cardiovascular system, which comprises the heart and a powerful network of bifurcating tubes: arteries, capillaries and veins. The heart through the rhythmic, pulsatile or periodic pumping action releases the fresh, oxygen and nutrient-rich blood into the arteries for onwards transmission to other parts of the body. The flow of blood in the arteries is affected by a number of factors: mechanical stress, geometric configuration, convections, its physiologic state (system resistances, venous pooling and intravascular blood volume), etc. The arterial responses to hemodynamic environment create normal adaptation or pathologic disease. Several pathological states may arise from excessive or uncontrolled responses to hemodynamic stimuli. Similarly, the effects of hemodynamics on convective mass transfer are great as most biologically active molecules such as nutrients, wastes, growth factors (hormones), and vasoactive compounds are carried from one site to another. Furthermore, the arterial blood flow is governed by the combined effects of the rhythmic pumping of the heart and the roles of thermal and concentration gradients due to the positive change in the environmental temperature and concentration conditions, and as such it is mixed convective.

A lot of research reports exist on this domain of study and other much related areas. For example, [1,2] studied the flow in branching cylindrical channels using the flow virtualization method, and observed that flow separations or reversals occur at the outside wall of the junction, especially when the flow rates in the daughter channels are different. Additionally, [3-18] studied experimentally, numerically or analytically the flow in bifurcating channels and arteries, and observed that increase in bifurcation angle increases the inlet pressure and consequently the velocity increases in the daughter channels. More so, [8] pointed out that the increase in bifurcation angle increases the wall shear stress. In other developments, [19] investigated experimentally the roles of waveforms on the flow distribution in cerebral aneurysms, and found among others, that a reduction in the pressure variable gives a universal relationship that characterized the flow; [20] studied the significance of surrounding tissues on the deformation and distensibility of both diseased and healthy arteries, and noticed that plagues reduce the distensibility of the arteries.

Moreover, the combined effects of magnetic field and convection in porous media flows in bifurcating and non-bifurcating channels have been studied. [21] investigated the flow in bifurcating fine capillaries using the simple perturbation series expansion, and found that the flow velocity decreases with the increase in the magnetic field but increases as the thermal parameters increase. [22] studied the magnetic field effects on the flow in a vertical rectangular channel using the method of perturbation series solutions, and observed that magnetic field parameter decreases the wall skin friction. Using experimental and finite difference numerical approaches [23] investigated a steady fully developed laminar flow through a pipe in the presence of magnetic field, and observed amongst others, that pressure is proportional to the flow rate, and the axial velocity reduces asymptotically as the Hartmann number becomes large; [16,24] considered the dynamics of a bifurcating river using the perturbation series solutions, and noticed that Grashof number increases the velocity, whereas Hartmann number and heat exchange parameter decrease it. [25] examined the oscillatory flow in a bifurcating green plant by perturbation series solutions approach, and saw that Heat exchange parameter, Peclet and Reynolds number increase the velocity factor.

Additionally, the flow of blood in the arteries under diseased state has been researched on. [26] examined the steady fully developed flow of blood in an atherosclerotic blood vessel with rigid permeable wall, and saw that the increase in the permeability of the blood vessel reduces the resistance due to stenosis; [27] investigated the pulsating flow of an incompressible viscous fluid through stenotic vessels using the Reynolds-averaged Navier-Stokes approach, and noticed that a wall shear stress peak occurred at the throat of the stenosis; [28] examined the effects of plague removal in small arteries using the method of numerical simulation, and observed that the removal of the plague leads to an increase in the flow rate of blood during the systole and diastole. Similarly, [29] examined the impact of heat and mass transfer on the flow of blood (which they considered as a Phan-Tien-Tanner fluid) through convergent-divergent tapering and non-tapering arteries for different parameters, and saw amidst others, that the shearing stress at the throat of the stenos increases with an increase in the external parameter, volumetric flow and Weissenberg number; [30] examined the roles of heat and chemical reactions on blood flow through an artery with overlapping stenosis, and noticed amidst others, that the coupling number, tapering angle, maximum height of stenosis, Sorret number or Brinkman number increases the axial velocity higher for the Newtonian fluid than for the micro-polar fluid. [31] considered blood flow through carotid bifurcating arteries clogged with fats using the one way fluid-solid interaction, and observed the effects of the Newtonian and non-Newtonian behaviorurs on the flow. [32] investigated the role of plaque removal on blood flow in a popliteal artery using experimental and numerical approaches, and observed that the removal of plaque increases the blood flow rate through the artery; there is a major reduction of pressure loss through the lesion. [33] studied analytically the transport of Low- Density Lipoprotein through an arterial wall under hyperthermia conditions using a four-layer model, and had results that are in excellent agreement with existing numerical and analytical literature data under isothermal conditions. [34] presented a flow model of blood under the influence of periodic acceleration through a multiple stenosed artery using the finite difference approach, and saw that the wall shear stress increases with Reynolds number. [35,36] considered the flow in a stenosed artery by a convergent-divergent description using the a modified simple perturbation method, and found

that the axial velocity and pressure are reduced through increasing the pulse amplitude and height of constriction, whereas the radial velocity and wall shear stress are increased as the pulse amplitude, height of constriction and Reynolds number increase. [37] considered blood flow through the arteries under atherectomy situation using an unsteady computational fluid dynamic solver, and found that the atherectomy procedure increases the flow through the stenos zone. [38] studied the flow of blood in a multi-stenosed artery using the a modified simple perturbation series expansion, and show that the axial pressure and radial velocity are decreased by increasing the amplitude; increase in the height of constriction increases the axial pressure but decreases the radial velocity; increase in the Reynolds number decreases the radial velocity.

[21] investigated the flow of blood in bifurcating fine capillaries wherein the inertia terms are zero. This work intends to extend [21] by allowing the inertia terms non-zero, and using the resulting models to examine the flow in a normal bifurcating artery.

This paper investigates the effects of magnetic field, heat exchange parameter, convection, bifurcation angle and Reynolds number on the flow dynamics of a normal bifurcating artery.

This paper is organized as follows: section 2 gives the methodology, section 3 holds the results and discussion, and section 4 bears the conclusion.

2. METHODOLOGY

We consider a model of the blood flow in a normal bifurcating artery. The problem is formulated on the assumption that: arteries are cylindrical, porous, axisymmetrically bifurcating and has negligible distensibility and tapered geometric effects; blood is homogeneous, chemically reacting but of the order one, and magnetically friendly due to its saline content; the flow is influenced by environmental temperature and concentration differentials, Earth and applied magnetic field, and heat source. Therefore, if (u', v', w') are the velocity components of the fluid in the mutually orthogonal (r', θ', x') axes, then the mathematical equations of mass balance/continuity, momentum, energy and diffusion governing the flow of the fluid in the presence of bifurcation angle, and considering the Boussinesq and Swell's free flow in vector form, become

$$\nabla.V' = 0 \tag{1}$$

$$\rho(V'.\nabla)V' = \nabla p' + \mu\nabla^2 V' + \rho g\beta_1(T' - T_\infty) + \rho g\beta_2(C' - C_\infty) - \frac{\mu}{\kappa}V' - \frac{\sigma_e B_o^2 V'}{\rho\mu\mu_m} \tag{2}$$

$$\rho C_p\left(V'.\nabla\right)\mathrm{T}' = k_o\nabla^2\mathrm{T}' + Q\left(\mathrm{T}' - \mathrm{T}_\infty\right) \tag{3}$$

$$\left(V'.\nabla\right)C' = D\nabla^2 C' + k^2{}_r\left(C' - C_\infty\right) \tag{4}$$

Assuming the velocity is symmetrical about the θ'-axis such that it is zero on the θ'-axis, the velocity components become (u', 0, w') in the orthogonal coordinates (r',0, x'). Then the models describing the flow in the dimensionless form are

$$\frac{1}{r}\frac{\partial(ru)}{\partial r} + \frac{\Re\partial w}{\partial x} = 0 \tag{5}$$

$$\frac{\partial^2 u}{\partial r^2} + \frac{1}{r}\frac{\partial u}{\partial r} - \frac{u}{r^2} = \frac{\partial p}{\partial r} \tag{6}$$

$$\frac{\partial^2 w}{\partial r^2} + \frac{1}{r}\frac{\partial w}{\partial r} - \left(M^2 + \chi^2 + \frac{\partial w}{\partial x}\right)w = \Re\frac{\partial p}{\partial x} - Gr\Theta - Gc\Phi \tag{7}$$

$$\frac{\partial^2\Theta}{\partial r^2} + \frac{1}{r}\frac{\partial\Theta}{\partial r} + N^2\Theta = Pe_h\left(u\frac{\partial\Theta}{\partial r} + \Re w\frac{\partial\Theta}{\partial x}\right) \tag{8}$$

$$\frac{\partial^2\Phi}{\partial r^2} + \frac{1}{r}\frac{\partial\Phi}{\partial r} + \delta_1^2\Phi = Pe_m\left(u\frac{\partial\Phi}{\partial r} + \Re w\frac{\partial\Phi}{\partial x}\right) \tag{9}$$

where

$$r = \frac{r'}{R_o}, x = \frac{\Re x'}{l}, w = \frac{w'R_o}{\upsilon}, \Theta = \frac{T' - T_\infty}{T_w - T_\infty}, \Phi = \frac{C' - C_\infty}{C_w - C_\infty},$$

$$p = \frac{(p' - p_\infty)R_o^3}{\rho l\upsilon}, \mathrm{Re} = \frac{Ul}{\upsilon}, M^2 = \frac{\sigma_e B_o^2}{\rho\mu\mu_m},$$

$$N^2 = \frac{Q}{k_o}, \chi^2 = \frac{R_o}{\kappa}, \delta_1^2 = \frac{k_r^2}{D},$$

$$Sc=\frac{\upsilon}{D},\Pr=\frac{\mu C_p}{k_o},Gr=\frac{g\beta_1(T_w-T_\infty)}{\upsilon^2},Gc=\frac{g\beta_2(C_w-C_\infty)}{\upsilon^2}$$

are the dimensionless quatities

Also, the geometry of the problem in Fig. 1 shows that the boundary conditions can be split into two distinct parts: the upstream/mother channel, $x<x$ and the downstream/daughter channel, $x>x_o$. Based on these, the boundary conditions are given as follows:

$$u=1,\ w=1,\ \Theta=1,\ \Phi=1 \quad \text{at} \quad r=0 \tag{10}$$

$$u=0,\ w=0,\ \Theta=\Theta_w,\ \Phi=\Phi_w \quad \text{at} \quad r=1 \tag{11}$$

for the upstream channel

$$u=0, w=0,\ \Theta=0,\ \Phi=0 \quad \text{at} \quad r=0 \tag{12}$$

$$u=0, w=0, \Theta=\gamma_1\Theta_w, \Phi=\gamma_2\Phi_w,\ \gamma_1<1,\ \gamma_2<1 \quad \text{at} \quad r=\Re\alpha x \tag{13}$$

for the downstream channel.

Additionally, for convenience, we assume the flow is fully developed such that $\frac{\partial u}{\partial r}=0$ [as cited in 39], and equations (5) - (9) are reduced to

$$\frac{\partial w}{\partial x}=0 \tag{14}$$

$$0=\frac{\partial p}{\partial r} \tag{15}$$

$$\frac{\partial^2 w}{\partial r^2}+\frac{1}{r}\frac{\partial w}{\partial r}-\left(M^2+\chi^2+\frac{\partial w}{\partial x}\right)w=\frac{\Re\partial p}{\partial x}-Gr\Theta-Gc\Phi \tag{16}$$

$$\frac{\partial^2\Theta}{\partial r^2}+\frac{1}{r}\frac{\partial\Theta}{\partial r}+N^2\Theta=Pe_h\Re w\frac{\partial\Theta}{\partial x} \tag{17}$$

$$\frac{\partial^2\Phi}{\partial r^2}+\frac{1}{r}\frac{\partial\Phi}{\partial r}-\delta_1^2\Phi=Pe_m\Re w\frac{\partial\Phi}{\partial x} \tag{18}$$

with the boundary conditions

$$w=1,\ \Theta=1,\ \Phi=1 \quad \text{at} \quad r=0 \tag{19}$$

$$w=0,\ \Theta=\Theta_w,\ \Phi=\Phi_w \quad \text{at} \quad r=1 \tag{20}$$

for the mother channel, and

$$w=0,\ \Theta=0,\ \Phi=0 \quad \text{at} \quad r=0 \tag{21}$$

$$w=0,\ \Theta=\gamma_1\Theta_w,\ \Phi=\gamma_2\Phi_w,\ \gamma_1<1,\ \gamma_2<1 \quad \text{at} \quad r=\Re\alpha x \tag{22}$$

for the daughter channel.

We seek for the solutions of equations (16)-(22) using the perturbation series expansion of the form

$$m(r,x)=m_o(r,x))+\xi m_1(r,x)+\xi^2 m_2(r,x)+... \tag{23}$$

where $\xi=\frac{1}{\mathrm{Re}}<1$ is the perturbation parameter. Furthermore, we adopt the expressions of the form: $g_0(r,x)=g_{00}(r)-\gamma x$ and $g_1(r,x)=g_{10}(r)-\gamma x$, where g_n represents the velocity, temperature and concentration in the upstream and downstream sections; and $p(x)=Kx-\frac{K_1x^2}{\Re}$, (where Kx is the pressure in the upstream, and $\frac{K_1x^2}{\Re}$ is that in the downstream). Using these in conjunction with equation (22) in equations (16)-(22), we have

$$\frac{\partial^2 w_{00}}{\partial r^2}+\frac{1}{r}\frac{\partial^2 w_{00}}{\partial r^2}-M^2w_{00}=\Re K-Gr\Theta_{00}-Gc\Phi_{00} \tag{24}$$

$$\frac{\partial^2\Theta_{00}}{\partial r^2}+\frac{1}{r}\frac{\partial\Theta_{00}}{\partial r}+N^2\Theta_{00}=-\gamma\Re Pe_h w_o \tag{25}$$

$$\frac{\partial^2\Phi_{00}}{\partial r^2}+\frac{1}{r}\frac{\partial\Phi_{00}}{\partial r}+\delta_1{}^2\Phi_{00}=-\gamma\Re Pe_m w_o \tag{26}$$

with the boundary conditions

$$w_{00}=1,\ \Theta_{00}=1,\ \Phi_{00}=1 \quad \text{at} \quad r=0 \tag{27}$$

$$w_{00}=0,\ \Theta_{00}=\Theta_w,\ \Phi_{00}=\Phi_w \quad \text{at} \quad r=1 \tag{28}$$

for the upstream channel, and

$$\frac{\partial^2 w_{10}}{\partial r^2}+\frac{1}{r}\frac{\partial^2 w_{10}}{\partial r^2}-M^2 w_{10}=\Re K_1 x-Gr\Theta_{10}-Gc\Phi_{10} \quad (29)$$

$$\frac{\partial^2 \Theta_{10}}{\partial r^2}+\frac{1}{r}\frac{\partial \Theta_{10}}{\partial r}+N^2\Theta_{10}=-\Re Pe_h\left(w_{00}\frac{\partial \Theta_{10}}{\partial x}+w_{10}\frac{\partial \Theta_{00}}{\partial x}\right) \quad (30)$$

$$\frac{\partial^2 \Phi_{10}}{\partial r^2}+\frac{1}{r}\frac{\partial \Phi_{10}}{\partial r}+\delta_1^2\Phi_{10}=-\Re Pe_m\left(w_{00}\frac{\partial \Phi_{10}}{\partial x}+w_{10}\frac{\partial \Phi_{00}}{\partial x}\right) \quad (31)$$

with the boundary conditions

$$w_{10}=0,\ \Theta_{10}=0\ ,\ \Phi_{10}=0 \quad \text{at} \quad r=0 \quad (32)$$

$$w_{10}=0,\ \Theta_{10}=\gamma_1\Theta_w,\ \Phi_{10}=\gamma_2\Phi_w,\ \gamma_1<1,\ \gamma_2<1 \quad \text{at} \quad r=\Re\alpha x \quad (33)$$

for the downstream channel, where $M_1^2=M^2+\chi^2-\gamma^2$

Furthermore, we define the associated Nusselt number (Nu), Sherwood number (Sh) and skin friction coefficient (WS), respectively as

$$Nu=-\left.\frac{\partial\Theta}{\partial r}\right|_{r=0},\ Sh=-\left.\frac{\partial\Phi}{\partial r}\right|_{r=0},\ WS=\left.\frac{\partial u}{\partial r}\right|_{r=0} \quad (34)$$

Now, the solutions of equations (24) – (34) are:

$$w_{00}(r)=PI_o(M_1 r)-\frac{1}{M_1^2}\Big[\Re K-Gr\left(LI_o\left(\sigma_+^{1/2}r\right)-\frac{K_v(r)}{\sigma_+}J_o\left(\sigma_-^{1/2}r\right)\right)-Gc\left(nI_o\left(\beta_+^{1/2}r\right)-\frac{K_w(r)}{\beta_+}J_o\left(\beta_-^{1/2}r\right)\right)\Big] \quad (35)$$

$$\Theta_{00}(r)=LI_o\left(\sigma_+^{1/2}r\right)-\frac{K_v(r)}{\sigma_+}J_o\left(\sigma_-^{1/2}r\right) \quad (36)$$

$$\Phi_{00}(r)=nI_o\left(\beta_+^{1/2}r\right)-\frac{K_w(r)}{\sigma_+}J_o\left(\beta_-^{1/2}r\right) \quad (37)$$

for the upstream channel, while

$$w_{10}(r)=tI_o(M_1 r)-\frac{1}{M_1^2}\Big[\Re K_1 x-GrqI_o\left(\sigma_+^{1/2}r\right)-\frac{K_y(r)}{\sigma_+}J_o\left(\sigma_-^{1/2}r\right)-Gc\left(sI_o\left(\beta_+^{1/2}r\right)-\frac{K_y(r)}{\beta_+}J_o\left(\beta_-^{1/2}r\right)\right)\Big] \quad (38)$$

$$\Theta_{10}(r)=qI_o\left(\sigma_+^{1/2}r\right)-\frac{K_y(r)}{\sigma_+}J_o\left(\sigma_-^{1/2}r\right) \quad (39)$$

$$\Phi_{10}(r)=sI_o\left(\beta_+^{1/2}r\right)-\frac{K_y}{\beta_+}(r)J_o\left(\beta_-^{1/2}r\right) \quad (40)$$

for the downstream channel

where $J_n(z)$ and $I_n(z)$ are the Bessel and modified Bessel functions of order n with the argument z, respectively.

3. RESULTS AND DISCUSSION

The flow problem of blood in a normal bifurcating artery is being considered. The effects of magnetic field strength, heat exchange parameter, Grashof number, bifurcation angle and Reynolds number are investigated. The results are obtained using Maple 18 computational software. For constant values of Pr =0.71, Re=0.03; γ_1 = 0.6, γ_2 =0.6, γ =0.7, Φ_w = 2.0, Θ_w =2.0 and varied values of M^2=0.1, 0.3, 0.5. 1.0, 5.0; N^2 = 0.1, 0.3, 0.5. 1.0, 5.0; Gr=0.1, 0.3, 0.5. 1.0, 5.0; α=5, 10, 15, 20 and Re=1000, 500, 50, 10 Tables 1-11 are obtained. The results show that the

- increase in the magnetic field strength increases the concentration but decreases the temperature, velocity and wall shear stress;
- increase in the heat exchange parameter increases the concentration and velocity;
- increase in the Grashof number increases the temperature, velocity, Nusselt number, Sherwood number and wall shear stress;
- increase in the bifurcation angle increases the temperature, velocity and wall shear stress;
- increase in the Reynolds number increases the concentration and velocity.

Blood is saline in nature. Therefore, it is electrolytic and exists as ions/charges. In a magnetic field, the motion of these ions produces electrical currents, which in turn are acted upon by the magnetic field to create a mechanical force (the Lorentz force) that gives the flow a new orientation. Usually, in many normal flow situations the Lorentz force has a freezing effect on the fluid motion. The higher the strength the weaker the velocity; see Table 3. Also, temperature, being velocity dependent and vice versa decreases with the velocity (see Table 1). More so, in a magnetic field, the chemical content of the fluid is fractionalized and polarized and tends to move towards the field. The magnetic field restraints the fluid from flowing out, thus increasing the concentration (see Table 2). These results are in perfect agreement with [16,22-24]. Similarly, the decrease in the velocity affects the stress on the wall in the downward trend (see Fig. 1).

Moreover, a temperature gradient exists between the ambient/equilibrium temperature and the environmental temperature. The positive environmental temperature may depend on the radiation from the sun or other heat sources. Higher environmental temperature creates room for heat absorption into the fluid. The absorbed heat energizes the fluid particles, looses them from the gripe of viscosity and makes them buoyant. This enhances the velocity and temperature of the fluid as seen in Tables 4 and 5. These results are in alignment with [25].

Similarly, the temperature or concentration gradient existing between the ambient temperature or concentration at r=0 and the positive environmental temperature or concentration situation in the presence of gravity, volumetric expansion and kinematic viscosity generates convective currents, which make the fluid buoyant and serve as lifting forces to the fluid particles. The energization of the fluid particles increases their kinetic energy, which enhances the velocity, as seen in Fig. 2. Furthermore, the increase in the fluid kinetic energy implies an increase in its temperature (see Tables 6 and 7). Additionally, the increase in the fluid temperature as shown in Tables 6 and 7 increases the rate at which heat is given

Table 1. Temperature distributions with variation in M^2 in the mother tube

r	M^2 =0.01	M^2 =0.1	M^2 =0.5	M^2 =1.0	M^2 =10.0
0.0	1.00000	1.00000	1.00000	1.00000	1.00000
0.2	1.33894	1.33353	1.25851	1.21973	1.18962
0.4	1.78420	1.78510	1.68302	1.53822	1.32604
0.6	1.80224	1.79844	1.77584	1.73913	1.71930
0.8	1.93941	1.81083	1.77981	1.76892	1.74411
1.0	2.00000	2.00000	2.00000	2.00000	2.00000

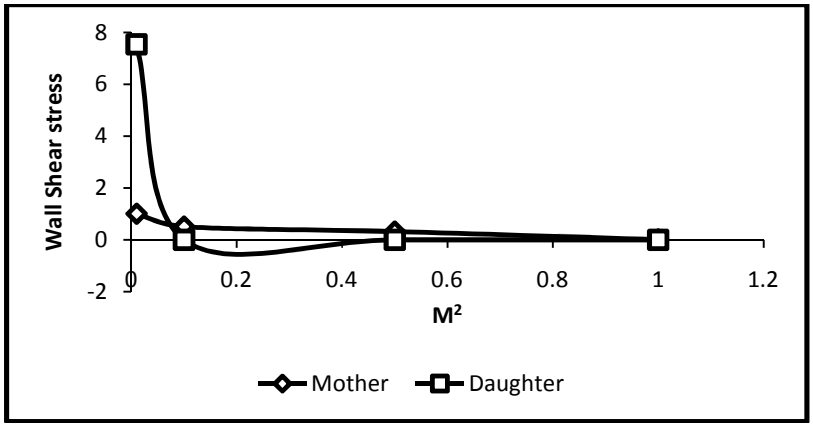

Fig. 1. Wall shear stress (Cf) for various magnetic field parameter (M^2) in the mother and daughter channels

out at the wall, provided the chemical reaction present in the system is not endothermic. Hence, the increase in the Nusselt number (see Fig. 3). In a similar manner, the increase in the rate of chemical interaction increases the Sherwood number, as seen in Fig. 3. Also, it is practically evident that the increase in the velocity as observed in Fig. 2 will increase the stress on the wall (see Fig. 4). These results are in consonance with [16,24].

Table 2. Concentration distributions with variation in M^2 in the daughter tube

r	M^2=0.01	M^2=0.1	M^2=0.5
0.0	0.00000	0.00000	0.00000
0.2	1.34194	1.74713	1.75971
0.4	0.93782	1.77142	1.85552
0.6	0.26574	1.81292	2.00874
0.8	0.68090	1.87344	2.24391
1.0	1.89381	1.95453	2.56703

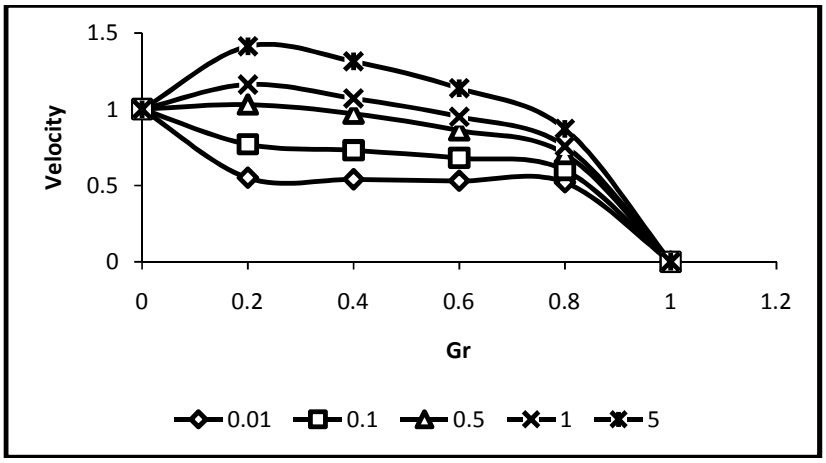

Fig. 2. Velocity-Grashof number profiles in the mother channel

Table 3. Velocity distributions with variation in M^2 in the mother tube

r	M^2 =0.01	M^2 =0.1	M^2 =0.5	M^2 =1	M^2 =10
0.0	1.00000	1.00000	1.00000	1.00000	1.00000
0.2	0.881703	0.811704	0.775002	0.713301	0.333304
0.4	0.781601	0.711702	0.680001	0.625001	0.031701
0.6	0.601701	0.543301	0.521604	0.493301	0.028301
0.8	0.346700	0.306704	0.296701	0.281704	0.018301
1.0	0.000000	0.000000	0.000000	0.000000	0.000000

Table 4. Concentration distributions with variation N^2 in the mother tube

r	N^2=0.01	N^2=0.1	N^2=0.5	N^2=1	N^2=10
0.0	1.00000	1.00000	1.00000	1.00000	1.00000
0.2	1.59431	1.59441	1.59459	1.59502	1.67101
0.4	1.86110	1.86124	1.86133	1.86201	1.95270
0.6	1.86294	1.91621	1.91642	1.91711	1.98060
0.8	1.97213	1.97221	1.97241	1.97313	1.98910
1.0	2.00000	2.00000	2.00000	2.00000	2.00000

Table 5. Velocity distributions with variation N^2 in the mother tube

r	N^2=0.01	N^2=0.1	N^2=0.5	N^2=1
0.0	1.00000	1.00000	1.00000	1.00000
0.2	0.962002	0.964001	0.984003	0.998902
0.4	0.631504	0.634503	0.648001	0.688504
0.6	0.321001	0.322001	0.330004	0.350001
0.8	0.009502	0.010004	0.018602	0.020103
1.0	0.000000	0.000000	0.000000	0.000000

Table 6. Temperature distributions with variation Gr/Gc in the mother tube

r	Gr=0.01	Gr=0.1	Gr=0.5	Gr=1	Gr=5
0.0	1.00000	1.00000	1.00000	1.00000	1.00000
0.2	1.05711	1.22503	1.41022	1.44813	1.69004
0.4	1.07320	1.35124	1.62781	1.67112	1.71614
0.6	1.55931	1.62141	1.85040	1.89391	1.91131
0.8	1.73393	1.80162	1.85911	1.94781	1.95362
1.0	2.00000	2.00000	2.00000	2.00000	2.00000

Table 7. Temperature distributions with variation in Gr/Gc in the daughter tube

r	Gr=0.1	Gr=0.5	Gr=1	Gr=5
0.0	0.000000	0.000000	0.000000	0.000000
0.2	0.982802	0.987501	0.990001	0.996804
0.4	1.75561	1.86394	1.984103	2.05741
0.6	2.98053	2.98981	3.00351	3.24190
0.8	4.00300	4.04271	4.09484	4.60493
1.0	5.05044	5.10723	5.18671	5.20490

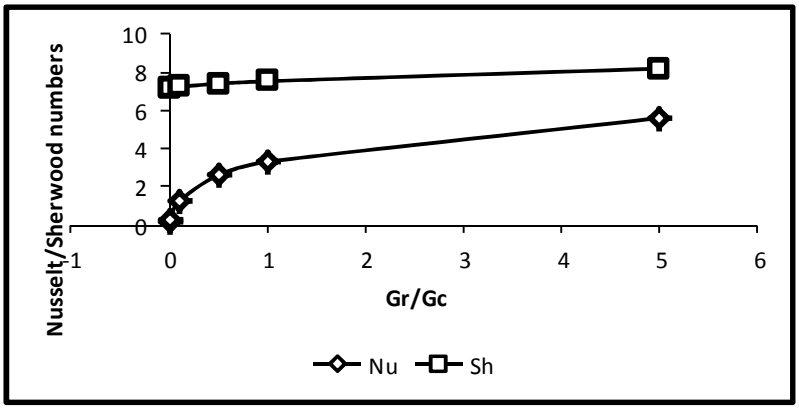

Fig. 3. Nusselt and Sherwood numbers-Grashof numbers profiles in the mother tube

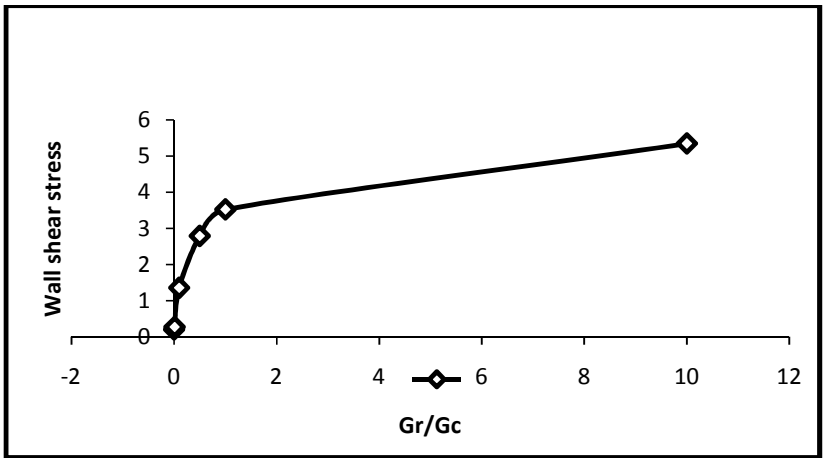

Fig. 4. Wall shear stress (WS)-Grashof numbers profile in the daughter channel

Naturally, the increase in bifurcation angle decreases the width of the daughter channel leading to an increase in the inlet pressure, which consequently increases the fluid velocity, as seen in Table 9. Furthermore, consequent upon the increase in the velocity produces a commensurate increase in the temperature (see Table 8). These results align with [3-18]. Also, other factors remaining constant, the increase in the velocity leads to increase in the wall shear stress, as shown in Fig. 5. This agrees with [8].

Table 8. Temperature distributions with variation in the bifurcation angle (α) in the daughter tube

r	α =5	α =10	α =15	α =20
0.0	0.000000	0.000000	0.00000	0.000000
0.2	1.10002	1.11002	1.1200	1.13503
0.4	2.20500	2.22004	2.23000	2.26502
0.6	3.31001	3.33001	3.36501	3.42004
0.8	4.44503	4.47004	4.49001	4.58003
1.0	5.60500	6.44001	5.70003	5.79001

Table 9. Velocity distributions with variation in bifurcation angle (α) in the daughter tube

r	α =5	α =10	α =15	α =20
0.0	0.000000	0.00000	0.000000	0.000000
0.2	1.13911	1.14834	1.16132	1.16800
0.4	1.13973	1.14731	1.15701	1.16031
0.6	1.14002	1.14633	1.15273	1.15633
0.8	1.14331	1.14552	1.15173	1.15531
1.0	1.14334	1.14450	1.15001	1.15430

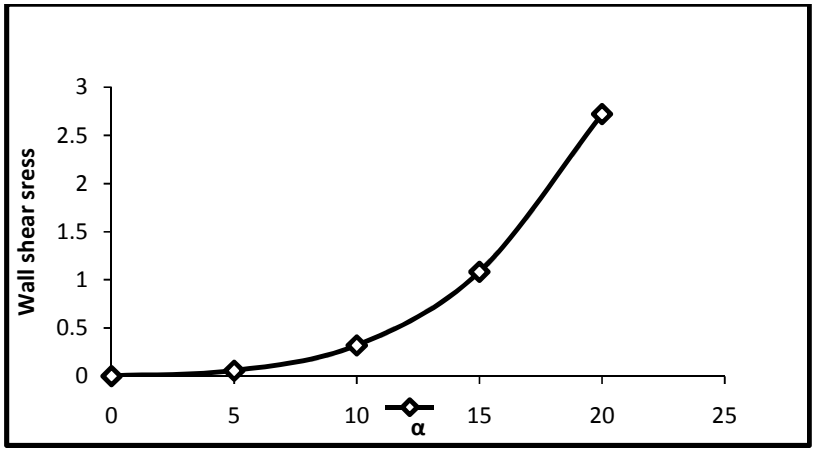

Fig. 5. Wall shear stress (WS) for various bifurcation angles (α) in the daughter channel

Table 10. Concentration distributions with variation in Reynolds number in the daughter tube

r	Re=500	Re=100	Re=50	Re=10
0.0	0.000000	0.000000	0.000000	0.000000
0.2	111.820	11.1830	0.111802	0.111302
0.4	781.532	78.1504	7.81504	0.787801
0.6	2214.10	221.411	22.1411	2.21411
0.8	5674.13	567.413	56.7413	5.67413
1.0	15780.1	1578.01	157.801	15.7801

Table 11. Velocity distributions with variation in Reynolds number in the daughter tube

r	Re=10000	Re=1000	Re=100	Re=10
0.0	0.000000	0.000000	0.000000	0.000000
0.2	342.283	34.2283	3.42283	0.342300
0.4	342.290	34.2270	3.42250	0.342401
0.6	342.364	34.2364	3.42364	0.342602
0.8	342.841	34.2861	3.42842	0.342904
1.0	343.603	34.3521	3.43503	0.343601

Even so, the flow in the mother tube is laminar; therefore its Reynolds number is moderate. But almost at the nodal point the inertia force rises due to a change in the geometrical configuration, thus leading to increase in the momentum and Reynolds number with subsequent increase in the velocity; see Table 11. Also, increase in the Reynolds number increases the mass-volume of the fluid transported, as depicted in Table 10. This agrees with [25].

The increase or decrease in the flow variables has some attendant health implications in man. In fact, the increase or decrease in the variables, especially concentration, temperature and velocity to levels beyond normal causes system malfunctioning, which is dangerous to his well-being. In particular, the decrease in the temperature and velocity due to the Hartmann number calls for a caution that people must not stay long under the influence of magnetic fields. On the other hand, the increase the flow variables within the naturally allowable levels accounts for a good distribution of blood and warmth round the body. And, this tends to enhance his physiologic well-being.

4. CONCLUSION

The flow of blood in a normal bifurcating artery is studied, and the effects of magnetic field, heat exchange parameter, convection parameter, bifurcation angle and Reynolds number are investigated. The results show that the increase in the

- Hartmann number increases the concentration but decreases the temperature, velocity and wall shear stress,
- heat exchange parameter increases the concentration and velocity,
- Grashof number increases the temperature, velocity, Nusselt number, Sherwood number and wall shear stress,
- bifurcation angle increases the temperature, velocity and wall shear stress,
- Reynolds number increases the concentration and velocity.

The increase and decrease in the flow variable have some health implications in man.

COMPETING INTERESTS

Authors have declared that no competing interests exist.

REFERENCES

1. Schroter RC, Sudlow MJ. Flow patterns in models of the human bronchial always. Respiratory Physiology. 1969;7:341-355.
2. Zellar H, Talukder N, Lorentz J. Model studies of pulsating flow in arterial branches and wave propagation in blood vessels. In fluid dynamics of circulatory flow. AGARD Conference Proceedings. 1970;65.
3. Pedley TJ, Schroter RC, Sudlow MF. The prediction of pressure drop and variation of resistance within the human bronchial airways. Respiratory Physiology. 1970;9: 387–405.
4. Lighthill MJ. Mathematical bio-fluid–dynamics Society for Industrial and Applied Mathematics, Philadelphia, Pennsylvania. 1972;19103:199–28.
5. Smith FT. Pipe flows distorted by non-symmetric indentation branching. Mathematika. 1976a;23:62-82.
6. Smith FT. On entry-flow effect in bifurcated blocked constricted tubes. Journal of Fluid Mechanics. 1976b;78:709–736.
7. Smith FT. Steady flow through a branching tube, Process Soc. London. 1977;A355: 167-187.
8. Pedley TJ. Pulmonary fluid dynamics. Annual Review Fluid Mechanics. 1977;9: 229–274.

9. Pedley TJ. The fluid mechanics of larger blood vessels Cambridge University Press, Cambridge; 1980.
10. Sobey J, Drazin G Philip. Bifurcating two-dimensional flow. Journal of Fluid Mechanics. 1986;171:263-287.
11. Smith FT, Jones MA. One-to-few and one-to-many branching tube flow. Journal of Fluid Mechanics. 2000;423:1–32.
12. Smith FT, Jones MA. Modeling of multi–branching tube flows: Large flow rates and dual solutions, IMA Journal of Mathematical Medical Biology. 2003; 20:183–204.
13. Smith FT, Ovenden NC, Frank P, Doorly DJ. What happens to pressure when a fluid enters a side branch. Journal Fluid Mechanics. 2003;479:231–258.
14. Tadjfar M, Smith FT. Direct simulation and modeling of basic 3-dimensional bifurcating tube flow. Journal Fluid Mechanics. 2004;519:1-32.
15. Bowles IE, Dennis SCR, Purvis R, Smith FT. Multi-branching flows from one mother tube to many daughters or to a network. Philosophical Transactions, Royal Society. 2005;A363:1015–1055.
16. Okuyade WIA, Abbey TM. A hydrodynamic model of flow in a bifurcating stream, part 1: Effects of bifurcation angle and magnetic field. Physical Science International Journal. 2016;12(1):1-13. DOI: 10.9734/PSIJ/2016/26410
17. Okuyade WIA, Abbey TM. Steady MHD fluid flow in a bifurcating rectangular porous channel. Advances in Research. 2016;8(3):1-17. DOI: 10.9734/AIR/2016/26399
18. Okuyade WIA, Abbey TM. Biomechanics of a bifurcating green plant, Part 1. Asian Journal of Physical and Chemical Sciences. 2017;1(2):1-22. DOI: 10.9734/AJOPS/2016/31458
19. Noel M Naughton, Brian D Plourde, John R Stark, Simona Hodis, John P Abraham. Impacts of waveforms on the fluid flow, wall shear stress, and flow distribution in cerebral aneurysms and the development of a universal reduced pressure. Journal of Biomedical Science and Engineering. 2014;7:7-14.
20. Sun BY, Vallez LJ, Plourde BD, Abraham, JP, Stark JR. Influence of supporting tissue on the deformation and compliance of healthy and diseased arteries. Journal of Biomedical Science and Engineering. 2015;8:490-499. DOI:http://dx.doi.org/10.4236/jbise.2015.88046
21. Okuyade WIA. MHD blood flow in bifurcating fine capillaries. African Journal of Science Research. 2015;4(4):56-59.
22. Abdel-Malek MB, Helal MM. Similarity solutions for magneto-force unsteady free convective laminar boundary–layer flow. Journal of Computation in Applied Mathematics. 2008;218:202–214.
23. Asadolah, Malekzadeh, Amir Heydarinasab, Bahram Dabir. Magnetic field effect on fluid flow characteristic in a pipe for laminar flow. Journal of Mechanical Science and Technology. 2011;25:333-339.
24. Okuyade WIA, Abbey TM. A hydrodynamic model of flow in a bifurcating stream, part 2: effects of environmental thermal differential. Physical Science International Journal. 2016;12(2):1-14. DOI: 10.9734/PSIJ/2016/26430
25. Okuyade WIA, Abbey TM. Steady oscillatory flow in a bifurcating green plant. Asian Research Journal of Mathematics. 2017;2(4):1-19. DOI: 10.9734/ARJOM/2017/31306
26. Das B, Batra RL. Non-Newtonian flow of blood in atherosclerotic blood vessel with rigid permeable walls. Journal of Theoretical Biology. 1995;175:1–11.
27. Varghese S, Franel S. Numerical analysis of flow through a severely stenotic vessel. Journal of Biomechanical Engineering. 2003;125:445-465.
28. Abraham JP, Sparrow EM, Lovik RD. Unsteady three-dimensional fluid mechanic analysis of blood flow in plaque-narrowed and plaque-free arteries. International Journal of Heat and Mass Transfer. 2008;51:5633-5641.
29. Noreen SA, Nadeen S, Changhoon L. Influence of heat and mass transfer on a Phan-Tien-tanner fluid model for blood flow through a tapered artery with a stenosis. 2012;7(43):3737-3750.
30. Mekheimer KhS, Haroun MH, El Kot MA. Influence of heat and mass transfer in blood flow throughan anisotropically tapered and elastic arteries with overlapping stenois. Applied Mathematical Information Science. 2012;6(2):281–292.
31. Pratumwal Y, Limtrakarn W, Premvaranon P. The analysis of blood flow past carotid bifurcation by using the one-way fluid-solid interaction technique (FSI). Transactions of the TSME. Journal of Research and

Applications in Mechanical Engineering. 2014;57-64.

32. Brian Plourde D, Lauren Vallez J, Biyuan Sun, John Abraham P, Cezar Staniloe S. The effect of plaque Removal on pressure drop and flow rate through an idealized stenotic lesion. Biology and Medicine; 2015.
DOI:http://dx.doi.org/10.4172/0974-8369.1000261
33. Marcello Iasiello, Kambiz Vafai, Assunta Andreozzi, Nicola Bianco. Low-density lipoprotein transport through an arterial wall under hyperthermia and hypertension conditions – An analytical solution. Journal of Biomechanics; 2015.
DOI:http://dx.doi.org/10.1016/j.jbiomech.2015.12.015
34. Satyasaran Changdar, Soumen De. Numerical simulation of nonlinear pulsatile newtonian blood flow through a multiple stenosed artery. International Scholarly Research Notices. 2015;1-11.
DOI: ttp://dx.doi.org/10.1155/2015/628605
35. Plourde BD, Vallez LJ, Sun B, Nelson-Cheeseman BB, Abraham JP, Staniloae CS. Alterations of blood flow through arteries following atherectomy and the impact on pressure variation and velocity. Cardiovasc. Eng. Technol. 2016;7(3):280-289.
DOI: 10.1007/s13239-016-0269-7
36. Okuyade WIA, Abbey TM. Oscillatory blood flow in convergent and divergent channels, part 1: effects of pulse amplitude and local constriction height. British Journal of Mathematics & Computer Science. 2016;14(6):1-17.
DOI: 10.9734/BJMCS/2016/23221
37. Okuyade WIA, Abbey TM. Oscillatory blood flow in convergent and divergent channels, part 2: Effects of Reynolds number. British Journal of Mathematics & Computer Science. 2016;15(1):1-14.
DOI: 10.9734/BJMCS/2016/23222
38. Okuyade WIA. Peristaltic transport with viscous dissipation effect in a multi-stenosed artery. Asian Research Journal of Mathematics 2017;5(2):1-18.
DOI: 10.9734/ARJOM/2017/31459
39. Zhong-Xian Yuan, Wen-Quan Tao, Qiu-Wang Wang. Numerical prediction for laminar forced convection heat transfer in parallel plate channels with stream-wise periodic rod disturbances. International Journal for Numerical Methods in Fluids. 1998;28(37):1371-1387

APPENDIX

$$K_v(r)=\frac{\sigma_-^{1/2}r^2}{2}\left\{-\gamma\Re^2 Pe_h K+\gamma\Re\varepsilon\left(1+\frac{\Omega_+ r^2}{4}\right)-\frac{\gamma\Re\varepsilon}{\Omega_+}K_u(r)\left(1-\frac{\Omega_- r^2}{4}\right)\right\}J_o\left(\sigma_-^{1/2}r\right)$$

$$K_u(r)=1-\frac{\gamma R^2\aleph^2}{2}\left(Pe_h+Pe_m\right)\left(r+\frac{\Omega_- r^3}{2}\right)$$

$$K_w(r)=\frac{\beta_-^{1/2}r^2}{2}\left\{-\gamma\Re^2 Pe_m+\gamma\Re\varepsilon\left(1+\frac{\Omega_+ r^2}{4}\right)-\frac{\gamma\Re\varepsilon}{\Omega_+}K_u(r)\left(1-\frac{\Omega_- r^2}{4}\right)\right\}$$

$$K_y(r)=\Big[1-\{-\gamma\Re\varepsilon Pe_h(K+K_1x)+\gamma\Re\varepsilon(\ LI_o\left(\Omega_+^{1/2}r\right)$$

$$-\frac{K_x(r)}{\Omega_+}J_o\left(\Omega_-^{1/2}r\right)+LI_o\left(\sigma_+^{1/2}r\right)-\frac{K_v(r)}{\sigma_+}J_o\left(\sigma_-^{1/2}r\right)+nI_o\left(\beta_+^{1/2}r\right)$$

$$-\frac{K_w(r)}{\beta_+}J_o\left(\beta_-^{1/2}r\right)\ )\ \}\frac{\sigma_-^{1/2}r^2}{2}\Big]$$

$$L=\frac{1}{I_o\left(\sigma_+^{1/2}\right)}\left[1+\frac{K_v(1)}{\sigma_+}J_o\left(\sigma_-^{1/2}\right)\right]$$

$$n=\frac{1}{I_o\left(\beta_+^{1/2}\right)}\left[1+\frac{K_w(1)}{\beta_+}J_o\left(\beta_-^{1/2}\right)\right]$$

$$P=\frac{1}{M_1^2 I_o(M_1)}\Big[\ \Re K-Gr\left(LI_O\left(\sigma_+^{1/2}\right)-\frac{K_v(1)}{\sigma_+}J_o\left(\sigma_-^{1/2}\right)\right)$$

$$-Gc(nI_o\left(\beta_+^{1/2}\right)-\frac{K_w(1)}{\beta_+}J_o\left(\beta_-^{1/2}\right))\ \Big]q=\frac{1}{I_o\left(\sigma_+^{1/2}\Re\alpha x\right)}\left[\gamma_1\Theta_w+\frac{K_y(\Re\alpha x)}{\sigma_+}J_o\left(\sigma_-^{1/2}\Re\alpha x\right)\right]$$

$$s=\frac{1}{I_o\left(\beta_+^{1/2}\Re\alpha x\right)}\left[\gamma_2\Theta_w+\frac{K_y(\Re\alpha x)}{\beta_+}J_o\left(\beta_-^{1/2}\Re\alpha x\right)\right]$$

$$t=\frac{1}{M_1^2 I_o\left(M_1\Re\alpha x\right)}\Big[\Re K_1x-Gr\left(qI_o\left(\sigma_+^{1/2}\Re\alpha x\right)-\frac{K_y(\Re\alpha x)}{\sigma_+}J_o\left(\sigma_-^{1/2}\Re\alpha x\right)\ \right)$$

$$-Gc\left(sI_o\left(\beta_+^{1/2}\Re\alpha x\right)-\frac{K_y(\Re\alpha x)}{\beta_+}J_o\left(\beta_-^{1/2}\Re\alpha x\right)\ \right)\ \Big]$$

$$\Omega_+=\frac{-\left(N^2-M_1^2\right)+\sqrt{\left(N^2-M_1^2\right)^2+4\left(N^2M_1^2+2\gamma\Re\varepsilon\right)}}{2}$$

$$\Omega_-=\frac{-\left(N^2-M_1^2\right)-\sqrt{\left(N^2-M_1^2\right)^2+4\left(N^2M_1^2+2\gamma\Re\varepsilon\right)}}{2}$$

$$\sigma_{+} = \frac{-\left(N^2 - M_1^2\right) + \sqrt{\left(N^2 - M_1^2\right)^2 + 4N^2 M_1^2}}{2}$$

$$\sigma_{-} = \frac{-\left(N^2 - M_1^2\right) - \sqrt{\left(N^2 - M_1^2\right)^2 + 4N^2 M_1^2}}{2}$$

$$\beta_{+} = \frac{-\left(\delta_1^2 - M_1^2\right) + \sqrt{\left(\delta_1^2 - M_1^2\right)^2 + 4\delta_1^2 M_1^2}}{2}$$

$$\beta_{-} = \frac{-\left(\delta_1^2 - M_1^2\right) - \sqrt{\left(\delta_1^2 - M_1^2\right)^2 + 4\delta_1^2 M_1^2}}{2}$$

$$\varepsilon = \gamma Pe_h Gr = \gamma Pe_m Gc$$

Peer-review history:
The peer review history for this paper can be accessed here:
http://sciencedomain.org/review-history/21260